7
Ultrashort optical pulses in time-varying medium

7.1 Introduction

Light behaves differently in a medium that changes with time. Optical pulses propagating through linear dispersive bulk medium do not undergo any temporal or spectral change when the entire dynamics remain time-invariant. On the other hand, the pulse dynamics become different than usual when they travel down a time-variant bulk medium. By the term time-variant we refer a medium having certain characteristic parameters being modulated with time. Pulse propagation through such a linear time-varying (or time-dynamic) system is an emerging field of research due to its potential applications in all-optical networks, optoelectronics, signal processing, pulse shaping and so on. Previously, it has been demonstrated in section 1.6 that an EM wave across a temporal boundary suffers a refraction phenomena in time, analogous to the spatial refraction, which ultimately leads to a temporal as well as spectral shift of light without any nonlinear intervention [Mendonça and Shukla, 2002]. The recent report by Xiao *et. al.* essentially agrees with the above notion by saying that optical pulses undergo temporal pulse shaping and an adiabatic wavelength shift while propagating through a time-varying linear medium [Xiao et al., 2011a]. Here, this study focuses on the behavior of optical pulses propagating from opposite directions in a linear medium whose refractive index is a function of time, i.e., $n = n(t)$ along with the effects of gain, loss, and dispersion. In general, the propagation of optical pulses in such time-varying media can be studied by solving the well-known Maxwell's equations using finite-difference time domain (FDTD) approach. However, to avoid the tedious process of FDTD, a new set of universal formulae, known as Time-transformation method (TTM), which is readily applicable to study the pulse propagation in a linear time-varying medium, has been implemented here.

In the subsequent sections of this chapter, the propagation dynamics of an ultrashort optical pulse having the shortest possible width has been investigated to cross the static temporal boundary in a linear medium from opposite direction. In section 7.2, a linear medium has been considered whose refractive index is time dependent as well as complex. With the imaginary part of the refractive index, an equal and adequate amount of gain–loss has been incorporated, such that the propagating pulse will experience the effect of a gain–loss-assisted media, though the net gain and loss of the system is zero. Pulse propagation in opposite directions has been studied in the said gain-loss-assisted time-varying linear medium resulting in asymmetric temporal and spectral shifts. Further, the behavior of such counter-propagating ultrashort pulses inside the linear gain-loss-assisted time-varying medium in the presence of dispersion has been studied. The effect of dispersion along with the effect of gain and loss has been studied in-depth. In section 7.3, a second set of investigation on the behavior of counter-propagating ultrashort pulses has been performed with a simple linear dispersive time-varying medium to explore the possibility of achieving certain amount of optical nonreciprocity in the dynamic system. It has been numerically shown that medium's dynamic refractive index changes the group velocity dispersion regime of the medium for

counter-propagating pulses. The non-identical dispersion regimes developed in opposite directions is understood to be a consequence of the system's broken time-reversal symmetry. Also, an asymmetric field-ratio of the output pulses indicates a nonreciprocal transmission. Moreover, pulses' spectral characteristics in opposite directions across the temporal boundary have found to be nonidentical indicating a phenomenon analogous to the unique spectral nonreciprocity which was previously observed in photonic crystals. It is to mention here that all the numerically estimated outcomes presented here have been supported by proper analytical calculations either using TTM or using basic principles of optics.

7.2 Asymmetric transmission of pulses in gain-loss-assisted time-varying medium

Asymmetric propagation of electromagnetic (EM) waves, unlike nonreciprocity, reverses the inherent properties of wave, depending on the direction of propagation. Such asymmetrical wave transmission is of immense interest due to its wide applicability in optoelectronic devices, signal processing etc. To date, asymmetric behavior of light was previously observed in various metamaterial based chiral waveguides and optical fibers. In the context of waveguides, diverse mechanisms have been exploited to achieve asymmetry such as, planar chirality of metamaterials along with loss incorporation [Fedotov et al., 2006], breaking of momentum symmetry at discontinuous phase interfaces [Xu et al., 2013], and breaking of polarization symmetry in hybrid plasmonic waveguide [Zhang et al., 2017]. For optical fibers, use of spiral fiber geometry have been helpful in breaking the directional symmetry of the fiber that leads to asymmetric polarization rotation of EM waves [Shemuly et al., 2013]. Moreover, use of active chiral metamaterials to dynamically control the wave propagation [Chen et al., 2017] and quantum inspired wave based system with exceptional singularities [Laha et al., 2018] are some new approaches to realize asymmetric wave propagation. Design and fabrication of prototypes in the context of optical isolators, circulators, and asymmetric mode converters are the rapidly evolving areas in integrated, all-optical applications that directly implement such asymmetric phenomena. However, all remarkable works on asymmetric light transmission are typically based on guided wave optics whereas, no such reports are available in literature that demonstrate asymmetric light transmission in bulk medium in device point of view. In this section, the potential use of the time-varying refractive index profile in a linear bulk medium, of any dimension and not constrained by a particular geometrical structure, to achieve asymmetric pulse propagation in both temporal and spectral domain will be demonstrated.

7.2.1 Pulse propagation in linear gain-loss-assisted dynamic medium

Here, the aim is to study the propagation of optical pulses through a non-dispersive gain-loss-assisted time-dynamic media. For this, a linear bulk medium has been considered in which the complex refractive index of the medium abruptly changes to some other value at a specific point of time. Moreover, same amount of gain and loss has been incorporated through the imaginary part of the complex refractive index into the medium, and is schematically depicted in figure 7.1. TTM, as described in section 2.2, has been implemented to investigate the interesting behavior of optical pulses through such unconventional optical configurations. Since TTM is applicable to all kind of pulse shape and duration, thus any standard optical pulse shape from commercially available laser sources can be chosen for the study of pulse propagation. Here, the evolution of a Gaussian pulse has been investigated during its propagation through the gain-loss-assisted time-dynamic system in counter-propagating directions. For numerical simulation, we have chosen the refractive indices n_1 and n_2 to be equal to the standard silica (R.I.=1.4446) and doped silica (R.I.=1.5980) glasses at the operating wavelength of 1.5 μm with equal amount of gain and loss of $\sim 10^{-6}$ having incorporated.

In figure 7.1, the vertical plane "B" is denoting the static temporal boundary where the refractive index is sharply changed to n_2 (step-like temporal index profile) from n_1. Moreover, vertical plane "A" and plane "C" are the two ends of the medium where the output pulses has been observed in case of counter-propagation. For ease of understanding of the results, we have considered the pulse propagation from left to right (denoted by the blue arrows) as forward and from right to left (denoted by the green arrows) as backward (Fig. 7.1).

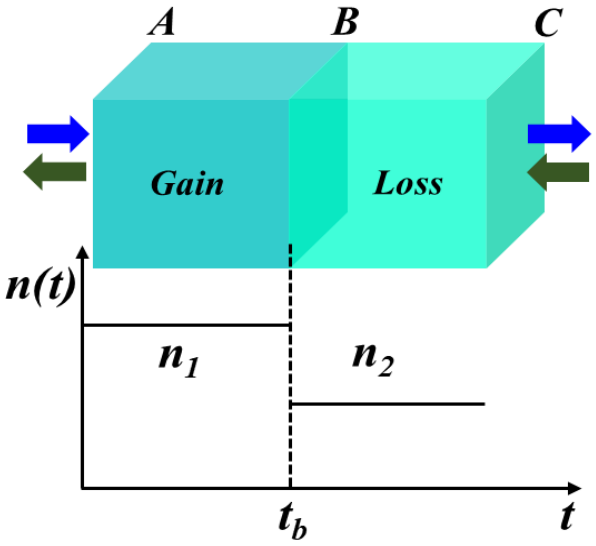

Figure 7.1: Schematic of the time-varying system with refractive index profile where t_b denotes the static temporal boundary coinciding with the vertical plane "B" of the bulk. Blue arrows denote the forward direction of pulse propagation while green arrows show backward propagation.

The universal formulas obtained using TTM both in time-domain and in frequency-domain has already been given by equations (2.82), and (2.83), respectively. The input pulse form has been chosen to be a standard Gaussian pulse given by,

$$E_{in}(t) = E_0 e^{-t^2/2T_0^2 - i\omega_1 t} \tag{7.1}$$

$$\widetilde{E}_{in}(\omega) = E_0 T_0 \sqrt{2\pi} e^{-T_0^2(\omega-\omega_1)^2/2} \tag{7.2}$$

where, E_0 denotes the initial pulse amplitude, ω_1 denotes the pulse central frequency, and T_0 is the pulse width. Further, the analytical expressions of the output temporal and spectral Gaussian pulse obtained through the universal formulas have been given by,

$$E_{out}(t) = sE_0 e^{-s^2(t^2-T_{d0})^2/2T_0^2 - is\omega_1(t-T_{d0})} \tag{7.3}$$

$$\widetilde{E}_{out}(\omega) = E_0 T_0 \sqrt{2\pi} e^{-T_0^2(\omega-s\omega_1)^2/2s^2 + i\omega T_{d0}} \tag{7.4}$$

where, s is the stretching factor, and T_{d0} denotes the effective transit time delay. Moreover, the complex refractive indices of the medium have been chosen to be of the form, $n_1 = n_{1r} + in_{1m}$ and $n_2 = n_{2r} - in_{2m}$ respectively, referring to the forward propagation. Here, the corresponding gain and loss have been incorporated through the imaginary parts n_{1m} and n_{2m} of the refractive index. Hence, the stretching factor s becomes $s = n_1/n_2 = s_r + is_m$ with s_r and s_m being the real and imaginary part of the stretching factor, and equation (7.11) has been modified to,

$$E_{out1}(t) = (s_r + is_m)E_0 \exp\big[(t - T_{d01})(\alpha_1(t - T_{d01}) + \beta_1) - i(t - T_{d01})(\alpha_1'(t - T_{d01}) + \beta_1')\big], \tag{7.5}$$

where $\alpha_1 = -(s_r^2 - s_m^2)/2T_0^2$, $\beta_1 = s_m\omega_1$, $\alpha_1' = s_r s_m/T_0^2$ and $\beta_1' = s_r\omega_1$. Moreover, T_{d01} denotes the effective transit time delay in forward propagation direction. From equation (7.5), the phase component of the output pulse has come out to be -

$$\phi(t) = (t - T_{d01})(\alpha'(t - T_{d01}) + \beta'), \tag{7.6}$$

which explicitly indicates a linear dependence of instantaneous frequency on time given as,

$$\delta\omega(t) = 2\alpha'(t - T_{d01}) + \beta'. \tag{7.7}$$

Further, considering the backward propagation of optical pulse, the successive refractive indices of the medium becomes, $n_1 = n_{1r} - in_{1m}$ and $n_2 = n_{2r} + in_{2m}$ and hence, $s = s_r - is_m$. Accordingly the output pulse form becomes,

$$E_{out2}(t) = (s_r - is_m)E_0 \exp\big[(t - T_{d02})(\alpha_2(t - T_{d02}) + \beta_2) - i(t - T_{d02})(\alpha_2'(t - T_{d02}) + \beta_2')\big] \tag{7.8}$$

where, $\alpha_1 = \alpha_2$, $\beta_1 = -\beta_2$, $\alpha_1' = \alpha_2'$ and $\beta_1' = -\beta_2'$, and T_{d02} denoting the effective delay during backward propagation. Similarly, the frequency-domain expressions for both the forward and the backward propagating pulses can be obtained as,

$$\widetilde{E}_{out1}(\omega) = E_0 T_0\sqrt{2\pi}\exp\big[-T_0^2(k\omega^2 + \omega_1^2 - l\omega\omega_1)/2 - i(\omega_1 T_{d01} + \omega(p\omega_1 + q\omega)T_0^2)\big], \tag{7.9}$$

$$\widetilde{E}_{out2}(\omega) = E_0 T_0\sqrt{2\pi}\exp\big[-T_0^2(k\omega^2 + \omega_1^2 - l\omega\omega_1)/2 - i(\omega_1 T_{d02} + \omega(p\omega_1 - q\omega)T_0^2)\big], \tag{7.10}$$

with $k = (s_r^2 - s_m^2)/(s_r^2 + s_m^2)^2$, $l = 2s_r/(s_r^2 + s_m^2)$, $p = s_m/(s_r^2 + s_m^2)$ and $q = s_r s_m/(s_r^2 + s_m^2)^2$.

Following the above analytical expressions, the pulse propagation has been observed in a semi-numerical approach in MATLAB®. For simulation, the initial pulse parameters are chosen to be, peak power (P_p) = 100 W, full-width-at-half-maximum (FWHM) = 1 ps, and maintained the same for the bi-directional propagations. The temporal output profiles for both forward and backward propagations are shown in figure 7.2. It is explicit from the figure that forward propagation has resulted in attenuation of the pulse whereas there is an adequate enhancement during backward propagation. Although, gain and loss has been incorporated in such a way that its effect will be canceled out in totality, however the real predicament is different from the previous notion.

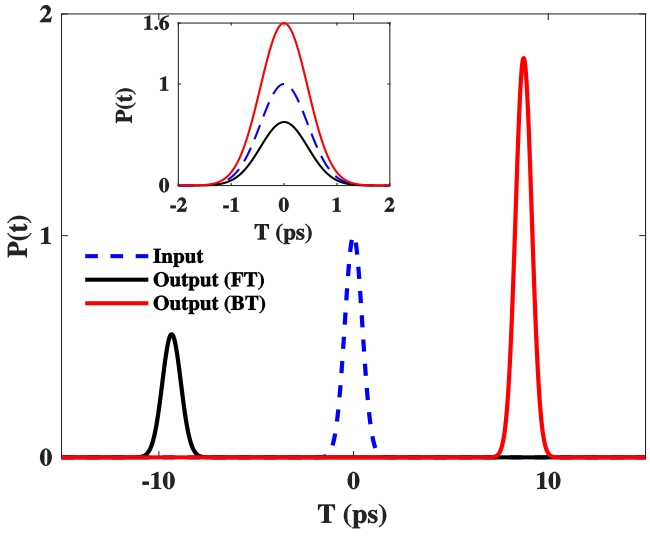

Figure 7.2: Time-domain input (dotted) and output pulse profile for forward (black) and backward (red) propagation in time-dynamic system. Inset shows the respective profiles for a time-static system.

Such enhancement or attenuation in power occurs entirely due to the temporal shifts of output pulses. As propagated down the system, pulses have been shifted from their initial center position where s_m is playing its dominant role. The respective shifts are in opposite sides of the initially fed pulse. In forward direction, T_{d01} = -9.3 ps, and in backward direction, T_{d02} = 8.7 ps, respectively. Moreover, reshaping of pulses can be understood as the presence of the ratio s. As reported by [Xiao et al., 2011a], pulse shape changes according to $s > 1$ or $s < 1$, and here also the reshaping depends on the real part of the complex ratio s_r i.e., either s_r is greater or less than 1 depending on the respective real values of the refractive indices. As stated before, the imaginary part of s i.e., s_m has the dominant role to play for any possible change in pulse shape. As the output pulse has shifted from $t = 0$ to $t = T_{d0}$, thus there is a large amount from s_m that is contributing to the exponent part of equation (7.11), which is positive for forward transmission and results in pulse attenuation, whereas negative s_m during backward transmission of light enhances the power. As estimated, nearly 44% of the input power has been attenuated during forward propagation through the system with its FWHM broadened by $\sim$ 13%, whereas backward transmission has enhanced the output power by 80% with 2% reduction in FWHM. Comparing the current results with that obtained for a system which is time-static but gain-loss assisted, pulse propagation is asymmetric only in terms of enhancement or reduction of power as no effective time delay will be observed. This is shown as inset of figure 7.2.

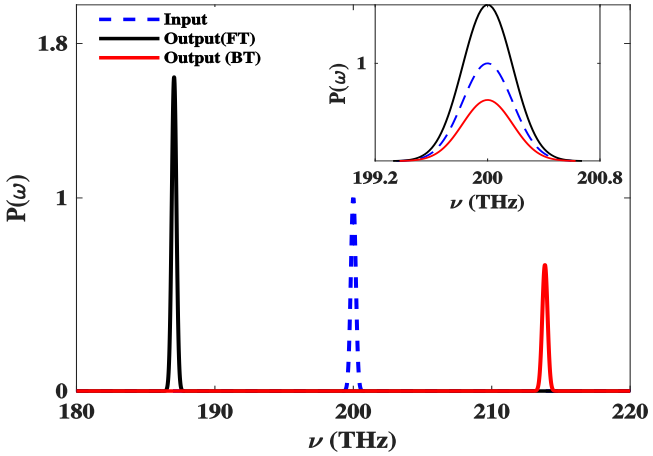

Figure 7.3: Input (dotted) and output spectra for both forward (black) and backward (red) propagation in time-dynamic system. Similar profiles for time-static medium are shown as inset.

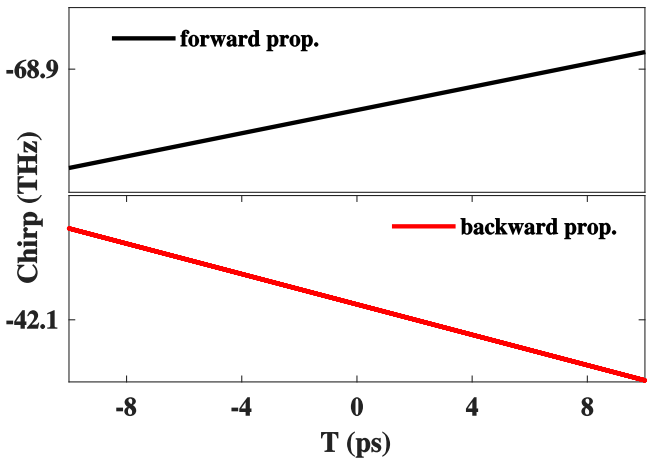

Figure 7.4: Variation of instantaneous frequency with time for both forward (black) and backward (red) propagation.

Accordingly, in frequency-domain the outputs for both the propagation directions are also shifted from the input spectrum centered at 200 THz ($\lambda = 1.5\mu$m) with its spectral FWHM $\sim$ 0.4 THz. While propagating in forward direction, output spectrum has been left-shifted by 12.9 THz from the initial center frequency, whereas 13.8 Thz shift towards right of the input frequency has been observed in opposite direction. Figure 7.3 clearly depicts the input and output spectra where the normalized spectral intensity has been plotted. It is to mention here that the phenomenon of spectral shift, as theoretically predicted, has been verified numerically through these observations. Unlike temporal profile, forward transmission has enhanced the spectral power by $\sim$ 60% with a spectral compression: output spectral FWHM = 0.32 THz, keeping the output energy content unchanged. Likewise, backward propagation has attenuated the intensity by $\sim$ 35% with spectral broadening: output spectral FWHM = 0.5 THz. Inset of figure 7.3 shows the spectral variation for time-static gain-loss assisted medium where no spectral shift has been observed. Further, according to equation (7.12) the accumulated phase variation shows quadratic behavior which leads to a linear frequency chirp (equation 7.5). The instantaneous frequency changes with time linearly with opposite slopes in opposite directions which corresponds to different signs of β_1' and β_2' and is depicted in figure 7.4.

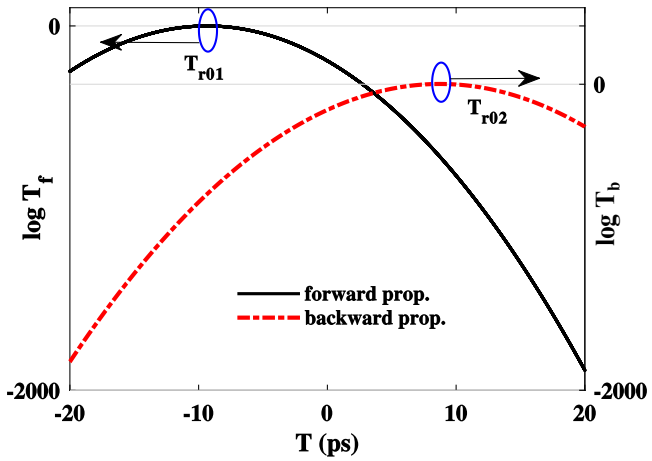

Figure 7.5: Logarithmic variation of forward transmission coefficient T_f and backward transmission coefficient T_b with related time-shift.

Further, to appreciate the asymmetric behavior of the pulses, the forward and backward transmission coefficients i.e., T_f and T_b respectively have been computed by the conventional expression of transmission coefficient $T = |E_{out}/E_{in}|^2$ and their logarithmic variation (i.e., $\log T_f$ and $\log T_b$) with time-shift have been shown. In this context, maximum of the transmission curve is found to be $2\log|s|$ which is time-independent and constant for a given system. In figure 7.5, $\log T_f$ and $\log T_b$ are plotted against time-shift which clearly shows that the transmissions in opposite directions are exactly opposite in nature. T_{d01} and T_{d02} are the respective effective time delays where the transmission curves reach their maximum i.e., the value of $2\log|s|$ is -0.134 at T_{d01} and 0.134 at T_{d02}.

This investigation has been extended further by increasing the number of time-boundaries with more than two changes of refractive index. In such case, s is the ratio of initial to final refractive indices and intermediate changes are accounted for the computation of effective time delay T_{d0}. It has been observed that for a configuration with even number of time-boundary, the propagation in opposite directions are symmetric with different T_{d0}, whereas odd number of time-boundaries lead to asymmetric propagation with different time-shifts. Moreover, with odd number of time-boundary the chirp is linear in both of the propagation directions, however even numbers do not show such linearity in chirp. We explain such behavior of pulse propagation depending on the number of

time-boundaries or refractive index changes as the consequence of presence of unequal refractive indices with gain-loss in the system. Even number of time-boundary leads to oppositely assisted end refractive index which leads to asymmetric propagation whereas odd numbered system starts and ends with similarly assisted refractive index (equal real and imaginary parts) as the initial, which lacks asymmetry.

7.2.2 Pulse propagation in linear dispersive gain-loss-assisted dynamic medium

In this subsection, the aim is to study the behavior of optical pulse propagation when the medium is linear, dispersive, and gain-loss-assisted time-varying one. As before, the refractive index of the linear bulk medium has been considered to be a function of time i.e., $n = n(t)$, and also a complex one. In figure 7.6, the schematic of the system is depicted along with its time-varying refractive index profile. The complex refractive index of the medium has been chosen to be of the form, $n = n_r \pm in_m$ where n_r is the real part, n_m the imaginary part, whereas the $\pm$ sign refers to loss and gain respectively. The refractive indices have been indicated by n_1 and n_2, respectively. The real part has been changed from n_1 to n_2 at a particular point of time t_b. In real structure, this change may occur in gradual manner. The imaginary part of the complex refractive index reflects the gain/loss incorporated into the system in equal amount such that it is an optically passive system. For forward propagation, the pulse will enter the system from the surface denoted by **A**, encounter the index change at **B**, and the output pulse detection will occur at the plane **C**. For backward propagation, the said path will be reversed.

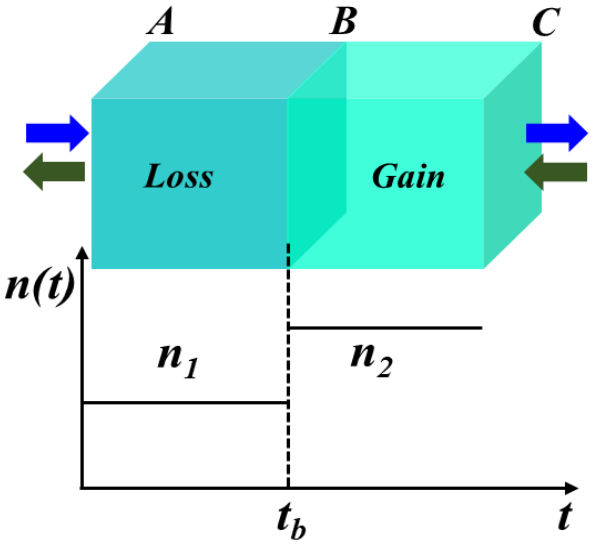

Figure 7.6: Schematic of the time-dynamic system along with the time-varying refractive index profile. n_1 and n_2 are the complex refractive indices and the change of index occurs at time t_b corresponding to the plane B. Blue arrow refers to forward propagation whereas green arrow indicates backward propagation of pulse.

A standard Gaussian pulse of the form given by equations (7.1) and (7.2) has been chosen to be the input to the dispersive bulk medium. Unlike the non-dispersive case, the problem in hand now has two parts - estimation of time-varying changes in the pulse, and the inclusion of dispersion effect to their dynamics. However, the system being a linear one, the analysis has been simplified by implementing separate operations for the time-transformation and the inclusion of dispersion, without loss of any generality [Xiao et al., 2012]. This approach is clearly depicted in figure 7.7. Following the process prescribed in figure 7.7, the first step has been to obtain the time-transformed

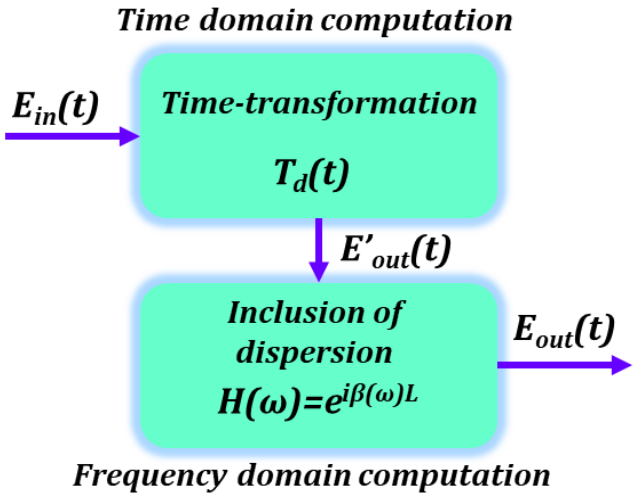

Figure 7.7: Block diagram of the analytical model used to solve numerically the pulse propagation through the linear time-dynamic system using time-transformation approach. $E_{in}(t)$ is the input pulse which initially will undergo only time-transformation technique. The intermediate output $E'_{out}(t)$ will then be treated in frequency domain to include the effect of dispersion. $E_{out}(t)$ is the final output.

output fields of the input Gaussian in time and frequency domain. By denoting the output fields by primed notation, the analytical forms of time-transformed Gaussian output is given by,

$$E'_{out}(t) = sE_0 e^{-s^2(t^2-T_{d0})^2/2T_0^2 - is\omega_1(t-T_{d0})} \tag{7.11}$$

$$\widetilde{E}'_{out}(\omega) = E_0 T_0 \sqrt{2\pi} e^{-T_0^2(\omega - s\omega_1)^2/2s^2 + i\omega T_{d0}} \tag{7.12}$$

where T_{d0} is the effective transit time delay and is computed from the relation given by equation (2.80). Moreover, the stretching factor s has been defined as the ratio of the initial refractive index n_1 to the final refractive index n_2 and takes the form $s = s_r \pm is_m$, where $\pm$ denotes the gain and loss, respectively.

To include the dispersion, it is important to know the frequency response function of the time-varying system. The total phase shift accumulated in the pulse at a particular frequency ω can be estimated by the relation, $\phi = \beta(\omega)L$ where a spatial length L can be considered to be the fixed spatial dimension of the bulk medium. Thus, the output spectrum with dispersion can be related to the time-transformed output spectrum by the equation -

$$\widetilde{E}_{out}(\omega) = \widetilde{H}(\omega)\widetilde{E}'_{out}(\omega) \tag{7.13}$$

where, $\widetilde{H}(\omega) = e^{i\beta(\omega)L}$ is the frequency response function of the linear dispersive time-varying medium under investigation. Moreover, $\beta(\omega)$ is the propagation constant of light pulse inside the medium which is related to the frequency dependent refractive index $n(\omega)$. Hence, as prescribed in section 2.2, $\beta(\omega)$ can be expanded in Taylor series around the carrier frequency ω_1 of the pulse, then it takes the form -

$$\beta(\omega) = \beta_0 + \beta_1(\omega - \omega_1) + \frac{1}{2}\beta_2(\omega - \omega_1)^2 + \dots \tag{7.14}$$

where terms up to second order of the expansion of $\beta(\omega)$ have been retained for the concerned bulk medium. Notably, β_0 is constant, β_1 the inverse of the group velocity of light, and β_2 accounts for the group velocity dispersion. The estimation of the output spectrum given by equation (7.13) has

been done in Fourier domain, and then the inverse Fourier transform has been done to obtain the time-domain output. After a rigorous exercise, the final analytical expressions have been obtained for the output pulse given by,

$$E_{out}(t) = \frac{E_0 T_0}{\sqrt{\frac{T_0^2}{s^2} - i\beta_2 L}} \exp\Big[\frac{(t - T_{d0} - \beta_1 L)}{2s(\frac{T_0^2}{s^2} - i\beta_2 L)}(-s^2(t - T_{d0} - \beta_1 L) - 2is\omega_1(T_0^2 - is\beta_2 L)) - \frac{\omega_1^2(T_0^2 - is\beta_2 L)^2}{2s(\frac{T_0^2}{s^2} - i\beta_2 L)} + i\beta_0 L - i\beta_1\omega_1 L + i0.5\beta_2\omega_1^2 L - 0.5T_0^2\omega_1^2\Big]. \quad (7.15)$$

From equation (7.15) using the expression $s = s_r \pm is_m$, the phase of the output pulse is obtained as-

$$\phi(t) = (t - T_{d0} - \beta_1 L)[a(t - T_{d0} - \beta_1 L) + b] + c \quad (7.16)$$

where, $a = \mp\frac{s_r s_m}{s(\frac{T_0^2}{s^2} - i\beta_2 L)}$, $b = -\frac{s_r\omega_1 T_0^2}{s(\frac{T_0^2}{s^2} - i\beta_2 L)}$ and $c = -\frac{s_r\beta_2\omega_1^2 L(\mp s_m\beta_2 L - T_0^2)}{s(\frac{T_0^2}{s^2} - i\beta_2 L)} + \beta_0 L - \beta_1\omega_1 L + 0.5\beta_2\omega_1^2 L$. The variation of instantaneous frequency over time is given by,

$$\delta\omega(t) = \frac{\partial\phi}{\partial t} = a(t - T_{r0} - \beta_1 L) + b \quad (7.17)$$

where, $\delta\omega(t)$ is the frequency chirp and is found to be linear over time.

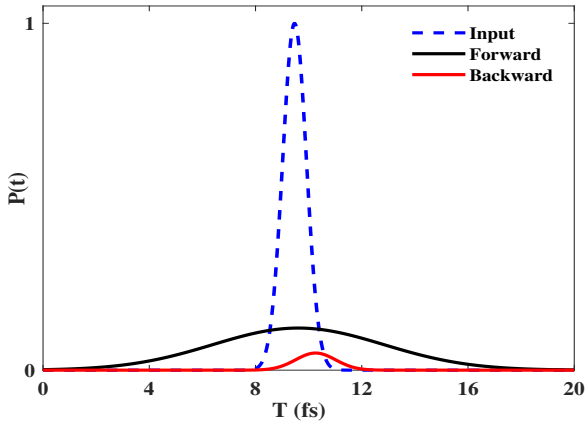

Figure 7.8: Variation of input (dotted) and output pulse profiles with time for forward and backward propagation directions.

The numerical simulation scheme of the analytical model is way too simpler by computing the time-transformation and dispersion separately. For simulation purpose, we have chosen the material of the system to be silica (r.i.=1.4446 at 200 THz) and doped silica (r.i.=1.5980 at 200 THz) where the step-like change in refractive index will be encountered at certain point t_b on the time axis. An equal amount of gain/loss of the order of 10^{-5} has been incorporated through the imaginary part of the refractive index. To study pulse propagation, a standard Gaussian pulse of peak power 100 W and full-width-at-half-maximum (FWHM) 1 fs centered at the frequency of 200 THz (corresponding wavelength = 1.5 μm) is considered as the input. Moreover, both the material and the time-dependent variations of refractive index has been accounted for the analysis of $\beta(\omega)$. The material refractive index variation over frequency have been computed by using well-known Sellmeier's equation, whereas the effect of the time-dependent refractive index profile has been incorporated by taking the Fourier transform of $n(t)$. Thus a combined $n(\omega)$ has been computed over the frequency range of ω corresponding to the temporal range t. Furthermore, β_0, β_1, and β_2

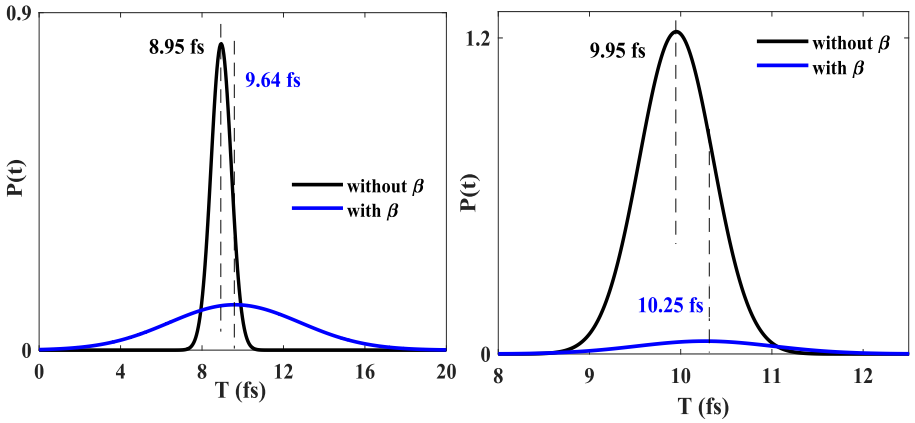

Figure 7.9: Temporal output pulse profile with and without the inclusion of dispersion effect for (a) forward and (b) backward propagation directions.

have been computed by their usual frequency dependent formulae. The corresponding values are as follows: in forward propagation, $\beta_0 = 5.46 \times 10^6$ m^{-1} , $\beta_1 = 4.34 \times 10^{-9}$ s/m, and $\beta_2 = 2.35 \times 10^{-24}$ s^2/m; in backward propagation, $\beta_0 = 4.25 \times 10^6$ m^{-1} , $\beta_1 = 3.38 \times 10^{-9}$ s/m, and $\beta_2 = -2.35 \times 10^{-24}$ s^2/m.

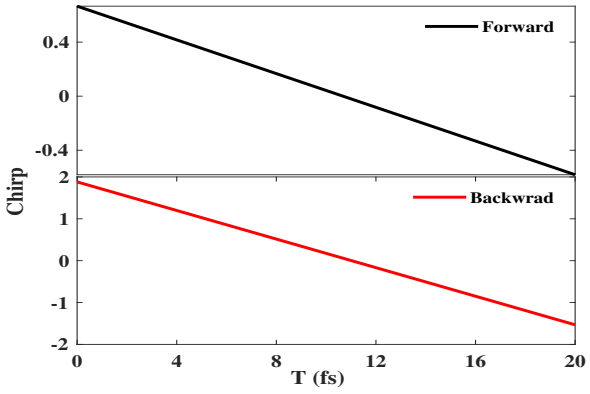

Figure 7.10: Variation of chirp with time during propagation in forward and backward direction.

The pulse propagation has been studied in counter-propagating directions i.e., from **A** to **C** referred as forward and **C** to **A** as backward. Output pulses from both of the propagations have been shown in figure 7.8 along with the input pulse (on shifted time axis to avoid negative time). It is clear from the figure that the output pulses in forward and backward propagation directions are completely different from each other. The amount of time-shift from the input in forward propagation is lesser than that in the backward propagation along with dissimilar reshaping of the pulses, which essentially shows an asymmetric behavior. The time-shift in forward propagation is 0.19 fs whereas in backward it is 0.80 fs. Moreover, there is a peak attenuation of $\sim$ 87% in forward propagation while backward propagation results in peak reduction by $\sim$ 95%. Both the peak attenuations correspond to broadening of the pulses with respect to the input; at **C** the pulse width has broadened to $\sim$ 7.8 fs whereas output at **A** has a FWHM of $\sim$ 1.8 fs. Such difference in output pulse parameters results from the two opposite dispersion regimes (normal and anomalous, respectively). In forward direction, the positive β_2 value, that corresponds to normal dispersion, reshapes the pulse in a way which is different from the effect of presence of negative β_2 value, that corresponds to anomalous dispersion, in backward direction which essentially makes the pulse

propagation asymmetric. It can be understood more clearly by comparing the output pulses with and without dispersion. Figures 7.9(a & b) clearly depict that there are two changes in the output with dispersion - one is the time-shift by the amount $\beta_1 L$, and the other one is the pulse shaping (or distortion) due to the GVD parameter β_2. Further, it has been found that the output chirp is linear and with similar slopes independent of the direction of propagation though with different amount. The chirp variation is depicted in figure 7.10 which states the asymmetric nature of pulse propagation through its amount of chirp developed.

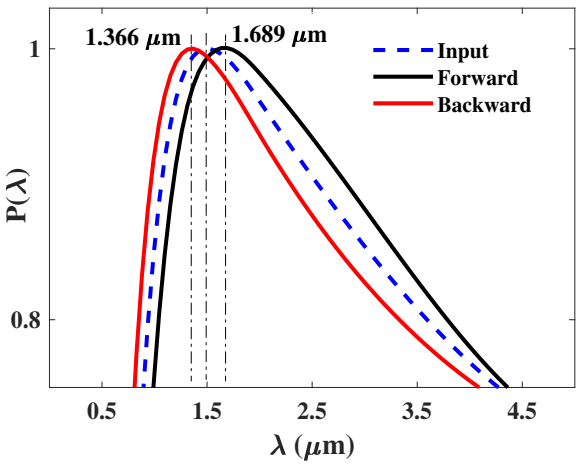

Figure 7.11: Variation of input (dotted) and output spectral intensity with wavelength for both forward and backward propagation.

The next interesting observation is the wavelength translation shown in figure 7.11. During forward propagation, the output spectrum is blue-shifted by ~ 0.19 μm from the central wavelength (1.5 μm) whereas in backward direction it is red-shifted by ~ 0.13 μm. Such observation is truly fascinating as the shift of light spectrum do not include any nonlinear process like four wave mixing but strictly dependent on the refractive index variation in a linear dispersive medium by an amount equal to $\mathbf{Re}[s\omega_1]$, i.e. as one varies the material index over time the s will be changed and the output range of wavelength will be varied accordingly. Thus we say that such translation is limited but tunable. Since the input pulse is a femtosecond one, thus the spectrum is largely broadened and most of the output spectral parts are overlapped with the input. As there is a shift in frequency, the peak intensity and width of the spectrum have been deviated from the input slightly, but scaled in a way to keep the total energy and the shape of the spectrum same. Since dispersion does not affect the shape of the pulse spectrum, thus the translation of wavelength with and without dispersion exactly overlaps.

In order to confirm the asymmetric behavior of pulse propagation, the transmission coefficient for both forward and backward directions have been computed using the conventional expression $T = |E_{out}/E_{in}|^2$. Figure 7.12 clearly depicts that the two transmissions are not same, neither they are overlapping on time axis nor they are mimicking each other in terms of amplitude. Such asymmetric nature of propagation can further be extended to establish optical non-reciprocity in dynamic photonic systems which may provide a new platform to control and manipulate light states. In the next section, the possibility of such linear dispersive time-varying medium to provide nonreciprocal transmission of light will be analyzed in the light of transfer function approach.

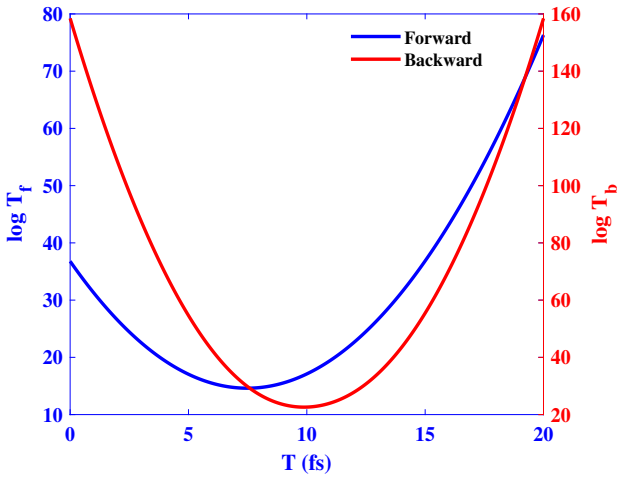

Figure 7.12: Transmission profiles corresponding to forward and backward propagation directions, respectively depicting the asymmetric nature of light propagation.

7.3 Towards optical nonreciprocity in time-varying medium

Optical nonreciprocity is widely established as an exclusive phenomena that breaks the Lorentz's reciprocity principle of certain photonic systems to block the undesired flow of light. There are always some practical situations where breaking of the device reciprocity is much required. For example, any back-reflected light, especially in lasers, in optical communication as well as in quantum computing and networks, affects the systems performance through unwanted optical interactions. To prevent such degradation, nonreciprocal optical devices such as isolators or circulators are usually employed between different parts of the all-optical network. In order to achieve this nonreciprocity in photonic devices, the basic requirement is to break the time-reversal symmetry (TRS) of the photonic system. A myriad of techniques have been explored till date to realize a broken TRS [Caloz et al., 2018]. The predominantly pursued technique has been to use strong external magnetic field to break TRS of magneto-optical materials. However, such conventional nonreciprocal devices are bulky and not compatible with the modern technological platform that eventually facilitate the demand of compact, integrable and low-cost systems. Fortunately, there are other approaches such as use of metamaterials [Mahmoud et al., 2015; Tan et al., 2019], space-time modulation [Taravati, 2018], nonlinearity induced spatial asymmetry [Laha et al., 2020], and photonic topological insulators [Rechtsman et al., 2013b] which have shown much potential to meet the current demand of advancing technology.

In this section, a lossless time-varying linear dispersive medium has been explored as a novel platform to realize nonreciprocal transmission of optical pulses via broken TRS. In the beginning of this chapter, the time-varying linear medium has been well-conceptualized to have a dynamic refractive index profile, and up to this point the asymmetric behavior of light pulses inside such medium has been demonstrated. However, realizing nonreciprocal transmission of light in such temporal boundary media, which can inherently break TRS, has not been explored yet, and will be presented in the subsequent sections.

7.3.1 Nonreciprocal nature of linear dispersive dynamic structure

In figure 7.13, the time-varying refractive index profile of the linear dispersive medium under investigation has been illustrated. The initial refractive index of the medium has been considered to be the refractive index of standard silica glass at 1.5 μm wavelength. In forward propagation

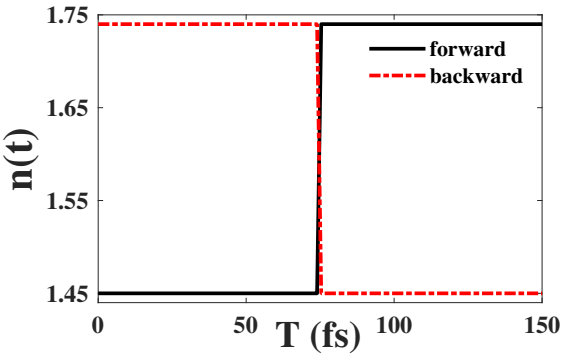

Figure 7.13: The time-varying refractive index profile for forward (blue) and backward (red) direction of propagation. The solid curves denote an abrupt change of index across the temporal boundary, whereas the dashed curves show their gradual change with time.

direction, the refractive index has been changed from n_1 to some higher value n_2 at a particular instant of time T, whereas in backward propagation the change has been from the higher to the lower value of refractive index at the same time instant. Thereby, a temporal boundary has been created within the time frame of the propagating pules. A relative change of refractive index in the form of $\Delta n/n$ has been considered where Δn and n are the amount of index change and the refractive index of the medium prior to the temporal boundary, respectively. Considering a single abrupt change of index from initial index value n_1, the final index value n_2 could be estimated by the relation,

$$n_2 = \left(1 + \frac{\Delta n}{n}\right) n_1. \tag{7.18}$$

Thus, the stretching factor $s = n_1/n_2$, where n_1 and n_2 are all real (lossless medium considered). For such linear time-varying medium, the output optical pulses can be easily obtained by using the universal formulas given by equations (2.82), and (2.83). An initial standard Gaussian pulse of the form,

$$E_{in}(t) = E_0 e^{-t^2/2T_0^2 - i\omega_1 t} \tag{7.19}$$

$$\widetilde{E}_{in}(\omega) = E_0 T_0 \sqrt{2\pi} e^{-T_0^2(\omega-\omega_1)^2/2}, \tag{7.20}$$

with amplitude E_0, pulse width T_0, and center frequency ω_1 has been treated with the time-transformation approach followed by the inclusion of dispersion by assuming the transfer function of the linear dispersive medium to be $H(\omega) = \exp[i\beta(\omega)L]$. However, in equation 7.14, we have considered terms up to second order only. As the pulse crosses the temporal boundary, the propagation constant changes by an amount proportional to the time-dependent change of refractive index Δn. Thus after the time boundary, $\beta(\omega)$ takes the form,

$$\beta(\omega) = \beta_0 + \beta_1(\omega - \omega_1) + \frac{1}{2}\beta_2(\omega - \omega_1)^2 + \Delta\beta(t) \tag{7.21}$$

where, $\Delta\beta(t) = (2\pi/\lambda)\Delta n$ [Plansinis et al., 2015]; λ is the wavelength of light. Since, the analytical formulation has already been presented in the previous sections, it's repetition will be unnecessary. Thus, it's convenient to jump straight to the Fourier domain analysis of the input and output pulses through the relation, $\widetilde{E}_{out}(\omega) = H(\omega)\widetilde{E}_{in}(\omega)$. After applying time-transformation and inclusion of dispersion, the input and the output pulse spectra in forward as well as in backward direction can

be written in the transfer matrix form as,

$$\begin{bmatrix} \widetilde{E}_{of}(\omega) \\ \widetilde{E}_{ib}(\omega) \end{bmatrix} = \begin{bmatrix} e^{m(\frac{1}{s_f^2}-1)+n(\frac{1}{s_f}-1)-i\omega_1 T_{df}+i\beta_f L} & 0 \\ 0 & e^{-m(\frac{1}{s_b^2}-1)-n(\frac{1}{s_b}-1)+i\omega_1 T_{db}-i\beta_b L} \end{bmatrix} \begin{bmatrix} \widetilde{E}_{if}(\omega) \\ \widetilde{E}_{ob}(\omega) \end{bmatrix} \tag{7.22}$$

$$\text{with,} \qquad m = -\frac{\omega^2 T_0^2}{2}, \qquad \text{and} \qquad n = \omega\omega_1 T_0^2,$$

where, $\widetilde{E}_{of}(\omega)$ and $\widetilde{E}_{if}(\omega)$ are the output and input spectra in forward propagation direction, respectively; $\widetilde{E}_{ob}(\omega)$ and $\widetilde{E}_{ib}(\omega)$ are output and input spectra in the backward propagation direction, respectively; s_f is the ratio of the refractive indices during forward propagation, whereas s_b is that in the backward propagation; T_{df} and $\beta_f(\omega)$ are the effective transit time delay and the propagation constant in the forward direction, respectively, whereas T_{db} and $\beta_b(\omega)$ are that in the backward direction of propagation. To obtain a quantitative idea of the nonreciprocal transmission, an expression of the scattering matrix for the dynamic medium has been curated through the transfer matrix of the same. One may write the transfer matrix T from equation (7.22) for the system concerned that relates the output fields of the system to the input fields by the expression,

$$T = \begin{bmatrix} T_{11} & T_{12} \\ T_{21} & T_{22} \end{bmatrix} = \begin{bmatrix} e^{m(\frac{1}{s_f^2}-1)+n(\frac{1}{s_f}-1)-i\omega_1 T_{df}+i\beta_f(\omega) L} & 0 \\ 0 & e^{-m(\frac{1}{s_b^2}-1)-n(\frac{1}{s_b}-1)+i\omega_1 T_{db}-i\beta_b(\omega) L} \end{bmatrix}. \tag{7.23}$$

Here, we have assumed the off-diagonal elements T_{12} and T_{21} to be zero based on the argument that for a temporal boundary there should always be a forward propagating light and no light can be reflected back in time. Thus, there should not be any light transmission in the backward direction from the temporal boundary. From the conventional relation of transfer matrix to scattering matrix, one obtains the elements of the scattering matrix for the time-varying medium as,

$$S = \begin{bmatrix} S_{11} & S_{12} \\ S_{21} & S_{22} \end{bmatrix} = \begin{bmatrix} 0 & e^{m(\frac{1}{s_b^2}-1)+n(\frac{1}{s_b}-1)-i\omega_1 T_{db}+i\beta_b(\omega) L} \\ e^{-m(\frac{1}{s_f^2}-1)-n(\frac{1}{s_f}-1)+i\omega_1 T_{df}-i\beta_f(\omega) L} & 0 \end{bmatrix}. \tag{7.24}$$

In equation 7.24 $s_f \neq s_b$, $T_{rf} \neq T_{rb}$, and $\beta_f(\omega) \neq \beta_b(\omega)$ (as shown in figure 7.14), thereby the two off-diagonal scattering matrix elements representing the transmission are also unequal, i.e. $S_{12} \neq S_{21}$. Therefore, according to the condition of nonreciprocity $S \neq S^T$. Further, the diagonal elements S_{11} and S_{22} representing the reflections of light are zero as obtained from the relations of S to T matrix. This can be well-understood by the previous argument for the temporal boundary where the reflected lights are a part of the transmitted light propagating in the same medium as the transmitted one but along a different trace, instead of being a back-reflected light in the previous medium as we observe in case of a spatial boundary.

The above analytical foundation has further been verified numerically by letting a Gaussian pulse having FWHM of 10 fs and peak power 1 W centered at ν=200 THz (corresponding to $\lambda = 1.5\mu$m) to propagate through the time-varying medium. A duration of 300 fs has been considered as the system dimension in time-scale corresponding to a spatial length $L = 2.5 \times 10^{-5}$m such that the pulse remains entirely inside the medium while crossing the temporal boundary. An entirely numerical approach has been opted to solve for the pulse propagation. The various dispersion coefficients in equation (7.21) such as β_0, β_1, and β_2 have been computed numerically by using their standard frequency dependent relations. In that case, the structural contribution of the frequency-dependent refractive index profile to the dispersion has been introduced by taking Fourier transform of the time-varying index $n(t)$ (as shown in figure 7.13). The variation of β with frequency ν (where,

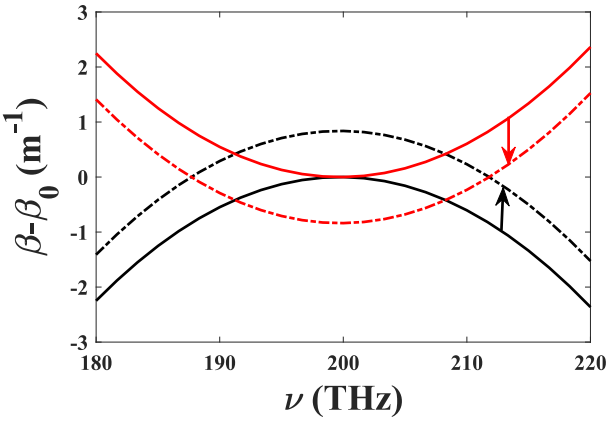

Figure 7.14: The variation of propagation constant β with frequency ν. The black and red solid curves show the variation of β in forward and backward propagation directions, respectively, before the time boundary. Similarly, the black and red dashed curves shows the same in forward and backward propagation directions, respectively, after the time boundary. The black and red arrows denote the change of β with time.

$\omega = 2\pi\nu$) has been depicted in 7.14 for both the forward and backward propagation directions (black and red solid curves, respectively) along with their respective variations before and after the time boundary (black and red dashed curves, respectively). It can clearly be seen that across the time boundary, the propagation constants for counter-propagating directions have changed by an amount equal to $\Delta\beta(t)$, and the corresponding shifts have been denoted by the black and red arrows. Moreover, they exhibit opposite signs throughout even after crossing the time boundary. Such similar kind of trend has been noticed for the estimated dispersion coefficients also. Interestingly, the simulated values of β_2 have been $\beta_{2f} = -7.07 \times 10^{-24}$ s^2.m^{-1}, and $\beta_{2b} = 4.72 \times 10^{-24}$ s^2.m^{-1}, where the f and b in suffices denote the forward and backward propagation directions. The opposite signs of the GVD parameter eventually enable the medium to operate in anomalous and normal regime of dispersion corresponding to the direction of propagation. This anomalous behavior of dispersion can be interpreted as the direct consequence of the medium's time-reversal symmetry breaking which essentially have led to switching of dispersion regimes on reversal of time, i.e. $\text{sgn}(\beta_2(T)) \neq \text{sgn}(\beta_2(-T))$.

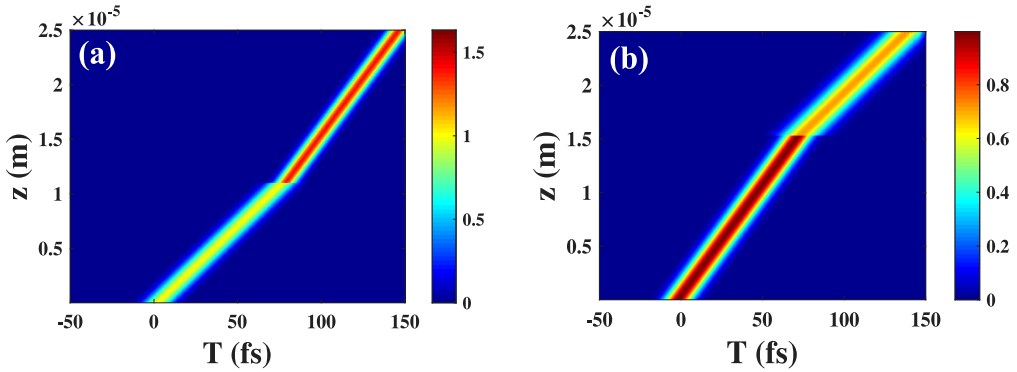

Figure 7.15: Time-domain evolution of the 10 fs Gaussian pulse in (a) forward direction, and (b) backward direction of propagation for a relative index change of 0.2; the propagation distance is the length that can be traversed by the pulse within its time frame.

Further, the evolution of the 10 fs pulse in accordance with forward index variation shown in figure 7.13 has been depicted in figure 7.15(a), whereas its propagation dynamics for backward

index profile has been depicted in figure 7.15(b). The temporal boundary occurs at ~ 75 fs where there is a sharp change in pulse width, amplitude as well as the path of evolution for which it comes out differently at the output end with the change in direction. For the forward index variation, the pulse gets compressed with a relative enhancement in amplitude, whereas it gets dispersed during transmission through the backward index profile. In addition, the time-reversal field-ratio of the counter-propagating pulses has also been estimated using the expression, P_{out}/P_{in} for both pulse propagation directions, where P_{out} and P_{in} are the output and input optical powers, respectively. According to [Fermann et al., 2000], an asymmetry in the time-reversal field-ratio signifies nonreciprocal property of the system. In forward transmission, the field-ratio has been obtained as 1.52, whereas during backward transmission, it has been 0.64. Moreover, we have quantified the degree of nonreciprocity by using the expression, $10\log_{10}[T_b/T_f]$, where T_b and T_f are the transmission coefficients in forward and backward directions, and have been estimated as $T = |E_{out}/E_{in}|^2$. For an abrupt change of refractive index corresponding to $\Delta n/n = 0.2$, the amount of nonreciprocity has been obtained to be $\sim$ -36 dB. It is to mention here that in figures 7.15(a) and (b), the trace of the reflected light is not present due to the fact that the TTM, in a straightforward way, gives the transmitted field profile without accounting for the reflected part of the light, which can be observed by solving the Maxwell's equations using FDTD approach.

7.3.2 Spectral nonreciprocity in time-varying media

A similar contrasting characteristic has been observed for the output spectral profiles of the counter-propagating pulses shown in figure 7.16(a). The input pulse spectrum has been shown in gray dashed curve, whereas the black solid and red dash-dotted curves are the output spectra for forward and backward propagating pulses, respectively. Interestingly, the output spectra have been shifted from their initial wavelength position resulting in contrasting spectral profiles at the output ends. From equation (7.22), one may observe clearly that the term $\pm n(1/s - 1)$ in the exponent introduces the spectral shift, which is also different for different values of s depending on the propagation direction. It is important to mention here that such contrasting spectra has been reported to be the essential feature observed in a time-varying medium. The previously observed wavelength translation also signifies the typical spectral nonreciprocity.

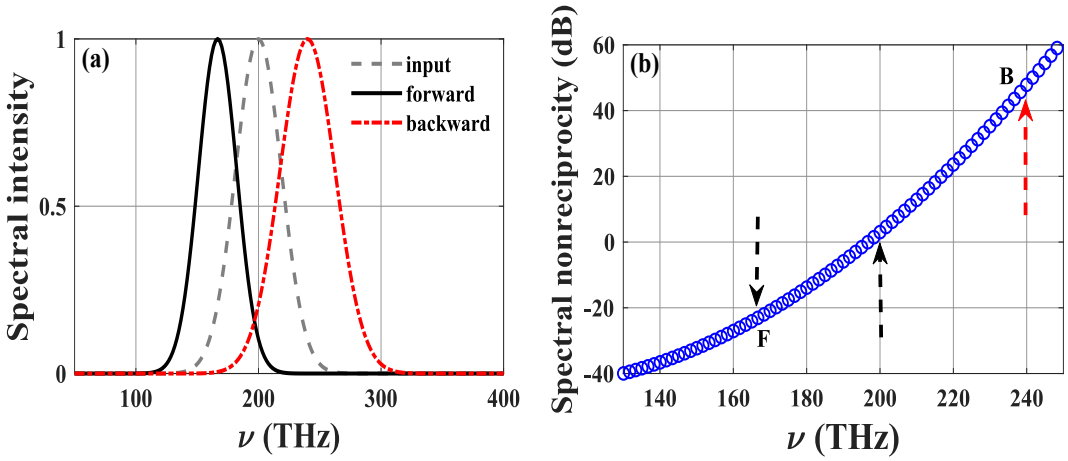

Figure 7.16: (a) The spectra of the 10 fs input Gaussian pulse (gray dashed), the output pulse in the forward propagation direction (black solid), and the output pulse in the backward direction (red dash-dotted). (b) The variation of spectral nonreciprocity measured in dB with frequency. The black arrow shows the input pulse frequency. **F** and **B** denotes the position of shifted frequencies in the forward and backward direction of propagation, respectively.

In addition, we have shown the degree of spectral nonreciprocity in figure 7.16(b), where

the ratio of spectral intensities of the two output spectra has been taken at each frequency ν in THz. For this study, we have used a 10 fs Gaussian pulse and kept $\Delta n/n$ at 0.2. Moreover, the calculation has been done over the frequency range of concern. The gray upward arrow in figure 7.16(b) denotes the input frequency of the pulse i.e. ν=200 THz, and the frequency points denoted by **F** and **B** are the locations of the two shifted spectral peaks during forward and backward propagation of light, respectively. At **F** the degree of nonreciprocity has been estimated as $\sim$ -23 dB, whereas at **B** it has been 47.8 dB. The change in sign is very much obvious as we have kept the ratio unchanged throughout, i.e. backward to forward. Also, a nearly 6 dB of nonreciprocity has been obtained at the initial frequency. Notably, the wavelength conversions earlier reported in [Notomi and Mitsugi, 2006; Xiao et al., 2011a] through various dynamic platforms was not associated with unidirectional transmission. However, in case of solid-state ring laser [Kravtsov et al., 2004] and magnetic photonic crystals [Sertel et al., 2011], which exhibit a unique dispersion relation $\omega(K) \neq \omega(-K)$, such spectral nonreciprocity has been observed leading to unidirectional light transmission. An analogous spectral behavior has been observed in linear time-varying medium which is the hallmark of the light refraction at the temporal boundary. It is noteworthy that the presence of spectral nonreciprocity in dynamic medium is unique and it has explicitly indicated towards the overall nonreciprocal behavior of the system.

7.4 Conclusions

In summary, a detailed numerical investigation has been performed to study the dynamics of ultrashort optical pulses inside a linear time-varying medium where the refractive index of the medium has been assumed to vary with time. A set of universal formulas, known as time-transformation method, has been implemented for both the analytical as well as semi-numerical estimation of the output pulses. Unlike FDTD, the time-transformation approach provides a faster and straightforward estimation process involving the electromagnetic field profiles only. The study has been done in three steps. First, a linear non-dispersive gain-loss assisted time-varying optical medium has been considered, and a complete asymmetric transmission of optical pulses in counter-propagating direction has been observed inside the system. A complex refractive index has been chosen as the time-dependent parameter in which the real part varies with time in a step-like manner and adequate, equal amount of loss/gain have been incorporated to the system through its imaginary part. It has been observed that the asymmetry occurs through two factors - one is the refractive index change with time that results in different time-delays, and other is the adequate amount of gain-loss that enhances the scaling of pulse amplitude. Second, the presence of dispersion has been considered in the previously studied linear, gain-loss-assisted time-varying medium, and a similar asymmetric behavior of optical pulse propagation along with a limited wavelength translation has been observed. A time-shifted dispersed output pulse has been obtained where the time-shift is dependent on propagation direction and reshaping of the pulse is due to opposite dispersion establishing the asymmetric nature. Moreover, there is a limited shift in wavelength which is also direction dependent and truly uncommon in such a linear system. Third, a linear gain/loss-less dispersive time-varying medium has been investigated to realize a novel mechanism for nonreciprocal transmission. Such a time-varying medium breaks the time-reversal symmetry of the system via refractive index change across the temporal boundary leading to a unique property of changing the dispersion regime in opposite propagation directions. This nonreciprocal behavior has been established systematically through numerical calculations of time-reversal field-ratios and the degree of nonreciprocity associated with the pulse propagation. A highly asymmetric time-reversal field-ratio along with a good amount of nonreciprocity has been achieved which quantify the strong nonreciprocal behavior of the dynamic medium. Moreover, an analytical approach has been implemented to obtain the asymmetric nature of the scattering matrix to support the argument of nonreciprocal behavior of light in the time-varying medium. Alongside, a contrasting spectral char-

acteristic, indicating a spectral nonreciprocity, of the counter-propagating pulses has been observed in this linear dynamic system. According to earlier reports, presence of such spectral nonreciprocity resulted from the optical nonreciprocity of the respective devices [Sertel et al., 2011; Kravtsov et al., 2004]. This statement subtly support the fact that the time-varying medium possibly will exhibit unidirectional light transmission.

7.4.1 Applications

It is strongly believed that such unconventional propagation behavior of light in the time-varying medium with further developments in this field will eventually reinforce novel optoelectronic devices for all-optical signal processing. It would readily facilitate the dynamic pulse shaping and the wavelength translation techniques based on linear processes only. A further in-depth study of such dynamic media will eventually develop novel nonreciprocal linear devices for all-optical networks.

7.4.2 Impact statement

The observations made in this chapter are very new, and their realization is straightforward from integrated optical device point of view with lesser complex working principle. The mathematical approach implemented in this study, namely the *time transformation method*, has provided an accurate estimation of the pulse behavior with much lesser computational complexity compared to other conventional approaches, which is considered as a novelty of this study. Further, we assume that the idea of having a time-varying refractive index in a waveguide will particularly be very interesting to study non-reciprocal light propagation through such a time-dependent system. A detailed scattering matrix approach has been adapted for the time-dependent linear problem to establish the nonreciprocal transmission of light, which has been performed for the first time in such time-varying system. Moreover, the results can be extended into waveguides, in which the refractive index can be modulated either by periodic and complex coupling between waveguides, driving different voltages along the waveguide length [Lira et al., 2012] in such a way to achieve the desired index profile, or by designing the waveguide in such a way that its refractive index will be periodically modulated [Nixon and Yang, 2015]. Light dynamics in time-varying systems is a broad domain of study which includes from various bulk dynamic media to dynamic waveguides, eventually developing a new platform for next-generation integrated all-optical devices.